

Cite this: *J. Mater. Chem. A*, 2022, 10, 14906

An amyloid-like proteinaceous adsorbent for uranium extraction from aqueous medium†

Qingmin Yang,^a Jian Zhao,^{*b} Arif Muhammad,^b Rongrong Qin,^b Juanhua Tian,^c Ling Li,^b Qianhui Zhang,^b Lixin Chen ^{*a} and Peng Yang ^{*b}

The most current developed uranium adsorbents usually suffer from relatively low adsorption capacity, poor selectivity, high cost, nondegradability and secondary environmental pollution issues. Therefore, it is urgent to develop an environmentally friendly bio-adsorbent with high adsorption performance and cost efficiency. Here, we prepare a proteinaceous adsorbent (phase-transitioned lysozyme- β -cyclodextrin, PTL- β -CD) through amyloid-like aggregation in aqueous solution under ambient conditions. The PTL- β -CD composed of micro-particles can effectively extract uranium ions from aqueous medium with a high adsorption ratio of 95.05%; and notably, the adsorption capacity per unit area is calculated to be $1.405 \text{ mg g}^{-1} \text{ m}^{-2}$, which is 3–90 times greater than that of the ion exchange resins, active carbon (AC), covalent organic frameworks (COFs) and metal organic frameworks (MOFs). High selectivity towards uranium ions in the presence of both common cations and anions is simultaneously obtained; In particular, the adsorption ratio is nearly 80 times higher than that of the competitive vanadium ions. It is demonstrated that the PTL- β -CD adsorbs uranium ions mainly through electrostatic interaction and surface complexation (*i.e.*, host-guest interaction between the hydrophobic internal cavities of β -CD and uranium ions, and metal chelation interaction between the surface hydroxyls of β -CD and uranium ions). Both lysozyme and β -cyclodextrin are cheap and easily available commercial chemicals, so the total cost of this proteinaceous adsorbent is only \$0.42 per g. Notably, the good biocompatibility and enzymatic degradability indicate that the PTL- β -CD is friendly to the environment and ecosystem. This novel green and facile approach shows great promise for the mass production of eco-friendly proteinaceous adsorbents to efficiently recover uranium ions from aqueous medium.

Received 23rd March 2022
Accepted 10th June 2022

DOI: 10.1039/d2ta02342c

rsc.li/materials-a

1. Introduction

As a typical low-carbon clean energy, nuclear power can effectively reduce environmental pollution caused by the consumption of fossil fuels.^{1–4} However, uranium has a limited reserve in terrestrial ore, and it will be exhausted some day. The total amount of uranium in seawater is ~ 4.5 billion tons, which is 1000 times more than that in land resources; in addition, there is also a considerable amount of uranium ions in nuclear industry wastewater. So the recovery of uranium from seawater or nuclear wastewater is a promising approach to make up for the uranium shortage and has attracted extensive attention

around the world.^{5–12} Among the various technologies and materials involved in uranium recovery, adsorption is the most attractive one because of its relatively easy operation and wide adaptability.^{13–15} At present, inorganic materials, organic polymers, carbon family materials and porous framework materials have been widely reported as uranium ion adsorbents, yet they usually suffer from poor selectivity, low adsorption capacity, an unclear adsorption mechanism, high cost, nondegradability and secondary environmental pollution issues.^{16–28} Even though some biomacromolecules such as DNA, super uranyl-binding proteins (SUPs), and peptides have been exploited to prepare high performance uranium ion adsorbents, their biodegradability is rarely mentioned; moreover, the acquisition of these raw materials is complicated and costly, and chemical cross-linking or special processing techniques must be undertaken, which impede their large-scale application.^{29–38} Therefore, it is highly desirable to develop a low-cost, easily fabricated, biodegradable and eco-friendly adsorbent to efficiently extract uranium ions from aqueous medium.

β -Cyclodextrin (β -CD) is a type of particularly interesting oligosaccharide molecule with a hydrophobic internal cavity

^aSchool of Chemistry and Chemical Engineering, Northwestern Polytechnical University, Xi'an 710072, China. E-mail: lixin@nwpu.edu.cn

^bKey Laboratory of Applied Surface and Colloid Chemistry, Ministry of Education, School of Chemistry and Chemical Engineering, Shaanxi Normal University, Xi'an 710119, China. E-mail: zhaojian@snnu.edu.cn; yangpeng@snnu.edu.cn

^cDepartment of Urology, The Second Affiliated Hospital of Xi'an Jiaotong University, West Five Road, No. 157, Xi'an 710004, China

† Electronic supplementary information (ESI) available. See <https://doi.org/10.1039/d2ta02342c>

and hydrophilic external surface.^{39–41} It can selectively chelate organic or inorganic compounds through its own polyhydroxy structure and host–guest interaction.^{42–45} Compared to other common metal ions, the β -CD exhibits superior adsorption and selectivity to uranium ions owing to the higher binding free energy.^{46,47} Accordingly, many β -CD based adsorbents have been of great interest and developed.^{48–50} The relatively good water solubility of β -CD certainly limits its application in metal extraction as an adsorbent individually; thus, β -CD must be combined with water insoluble carriers, including carbon nanotubes, graphene oxide, graphene aerogel, graphite carbon nitrogen (g-C₃N₄), PAN membranes, magnetic iron oxide, Al(OH)₃, titanium dioxide, montmorillonite and so on,^{46,47,51–60} with the aim to isolate metal loaded adsorbents from solution. Even though these β -CD based adsorbents present good adsorption capacity and selectivity for uranium ions, the preparation process is complicated, and toxic organic reagents are often required; besides, water insoluble carriers are costly, non-renewable and nondegradable. The above disadvantages heavily limit their large-scale application and may also further lead to secondary ecosystem pollution. Alternatively, lysozyme is a very cheap water-soluble globular protein, and it can be extracted in large quantities from egg whites and has been widely used as food additives and biomedical antibacterial agents.^{61–63} In our previous work, we found that lysozyme could undergo a fast phase transition process in a few minutes with a disulfide breaker tris(2-carboxyethyl)phosphine (TCEP) in an aqueous solution. During the phase transition process, the partially unfolded protein monomers self-assembled into solid aggregates with an internal amyloid-like structure in the bulk solution.^{64–66} A large number of amino acid residues such as carboxyl, amino, hydroxyl, sulfhydryl, and imidazole existing on the surface of lysozyme aggregates can provide active binding sites for interacting with metal ions through electrostatic interaction and complexation, which makes them a kind of potential adsorbent for metal ion extraction.^{67,68} However, the adsorption capacity and selectivity of lysozyme aggregates towards uranium ions are severely restricted due to the lack of specific adsorption active sites. Owing to the robust β -sheet stacking inner structure, the solid aggregates exhibit excellent structural stability in harsh physical and chemical environments, and they are accordingly estimated to have good adaptability and durability in metal ion adsorption; otherwise, they can be degraded by trypsin and pepsin as well, which is beneficial for reducing the secondary environment pollution usually caused by polymeric adsorbents.^{69–76} Consequently, taking full advantage of the distinctive features of β -CD and lysozyme, we developed a novel uranium ion bio-adsorbent based on lysozyme- β -cyclodextrin conjugates through a facile amyloid-like aggregation method. The lysozyme- β -cyclodextrin conjugates (Ly- β -CD) were synthesized first by the reaction of an amine with an *N*-succinimidyl activated ester, and then the conjugates underwent a phase transition process in aqueous solution rapidly to form solid PTL- β -CD aggregates. The prepared PTL- β -CD aggregates can extract uranium ions from aqueous medium with a high adsorption capacity per unit area of 1.405 mg g⁻¹ m⁻², and are superior to the general adsorbents

such as AC, resins, MOFs, and COFs; meanwhile, they also exhibit high uranium ion selectivity in the presence of various common cations (*e.g.*, VO²⁺, Cr³⁺, Fe³⁺, Mn²⁺, Ni²⁺, Pb²⁺, Cd²⁺, Co²⁺, Mg²⁺, As³⁺, K⁺, Ca²⁺, and Na⁺) and anions (*e.g.*, Cl⁻, CO₃²⁻, SO₄²⁻ and NO₃⁻). The effects of adsorption conditions (*e.g.*, solution pH, initial uranium ion concentration, and temperature) on adsorption performance were investigated. The analysis of kinetic and thermodynamic models suggested that the adsorption is a spontaneous, endothermic and monolayer chemisorption process. The efficient adsorption and outstanding selectivity of PTL- β -CD were mainly attributed to host–guest interaction (between the hydrophobic internal cavities of β -CD and uranium ions) and metal chelation (between the surface hydroxyls of β -CD and uranium ions). Moreover, the good biocompatibility and biodegradability of PTL- β -CD characterized by cytotoxicity and enzymatic hydrolysis tests indicated its environmental friendliness. The inexpensive raw materials and green preparation process provide the possibility for the development and large-scale application of the proteinaceous uranium adsorbent.

2. Results and discussion

2.1. Preparation and characterization of the lysozyme- β -CD conjugates

As shown in Fig. 1a, hydroxypropyl- β -cyclodextrin (Hp- β -CD, $M_w = 1500$, Fig. S1†) was first activated by *N,N'*-disuccinimidyl carbonate (DSC) to form *N*-hydroxysuccinimide-functionalized β -CD (NHS- β -CD); then the lysozyme- β -cyclodextrin conjugates (lysozyme- β -CD) were synthesized through the reaction of an amine with an *N*-succinimidyl activated ester under ambient conditions. The reaction product was characterized by Fourier transform infrared spectroscopy (FTIR), X-ray photoelectron spectroscopy (XPS), and matrix-assisted laser desorption ionization time-of-flight mass spectrometry (MALDI-TOF). Fig. 1b shows the FTIR spectra of β -CD, lysozyme, and lysozyme- β -CD, respectively; the appearance of a new peak at 1030 cm⁻¹ corresponding to the C–O stretching vibration of β -CD indicates the successful grafting of β -CD onto lysozyme, which is also verified by the XPS results in which the C–OH content in lysozyme- β -CD is significantly higher than that in lysozyme (Fig. 1c). In addition, it is calculated from the molecular weights in the MALDI-TOF results that nearly 1 ~ 3 β -CD molecules have been grafted onto one lysozyme molecule (Fig. 1d). Previous studies have demonstrated that the essence of superfast protein amyloid-like aggregation is the transformation of the secondary structure of protein from α -helix to β -sheet;^{66,70,76} it is therefore necessary to check whether the chemical grafting process and the grafted β -CD could change the secondary structure of lysozyme. As shown in Fig. 1e, the far-UV circular dichroism (far-UV CD) curves of native lysozyme and lysozyme- β -CD are highly identical with two α -helical peaks at 208 nm and 222 nm, suggesting no distinct difference between their secondary structures. Moreover, the bactericidal activity of β -CD, native lysozyme, and lysozyme- β -CD was evaluated, and the results displayed in Fig. S2† indicate that the β -CD conjugation causes almost no changes in the three-dimensional structure of

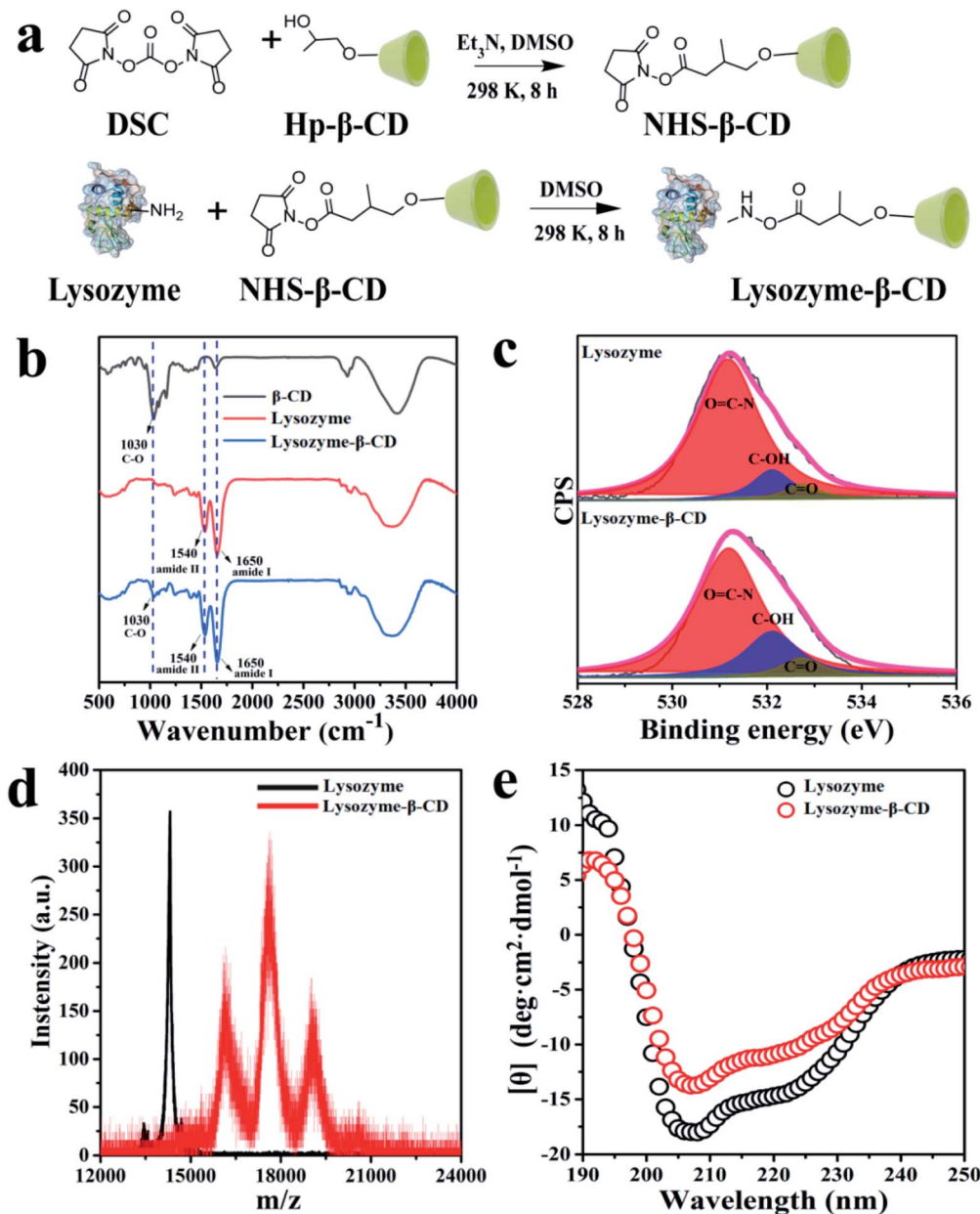


Fig. 1 Preparation and characterization of the lysozyme- β -CD conjugates. (a) Synthetic route of lysozyme- β -CD conjugates. (b) FTIR spectra of β -CD (black), lysozyme (red) and lysozyme- β -CD (blue), respectively. (c) High-resolution O_{1s} XPS spectra of lysozyme and lysozyme- β -CD. (d) MALDI-TOF spectra of lysozyme (black) and lysozyme- β -CD (red). (e) Far-UV CD spectra of lysozyme (black) and lysozyme- β -CD (red).

lysozyme molecules; otherwise the activity of the lysozyme- β -CD conjugate will be reduced. In fact, the antibacterial activity of lysozyme- β -CD conjugates is even higher than that of lysozyme (Fig. S2[†]), which is possibly due to the hydrophobic cavity in β -CD increasing the hydrophobicity of the conjugates.^{77,78}

2.2. Preparation and characterization of the PTL- β -CD aggregates

For the native lysozyme, the reducing agent TCEP can break the disulfide bonds that stabilize its spatial structure resulting in protein partial unfolding and exposure of the internal hydrophobic groups. Subsequently, the resultant unfolded

monomers can rapidly transform into β -sheet stacking-based amyloid-like oligomers which finally form aggregates composing of microparticles in bulk solution (also called phase-transited lysozyme, PTL) driven by hydrophobic forces.^{63,64} As discussed above, the lysozyme- β -CD conjugate maintained almost the same three-dimensional structure with native lysozyme (Fig. 1e), and it is reasonable to suppose that the lysozyme- β -CD conjugate can also undergo a similar phase transition process upon reacting with TCEP to form solid PTL- β -CD aggregates (Fig. 2a). In order to test the above speculation, the breakage of disulfide bonds in the lysozyme- β -CD conjugates was detected by *N*-(1-pyrenyl)maleimide (NPM) staining. The

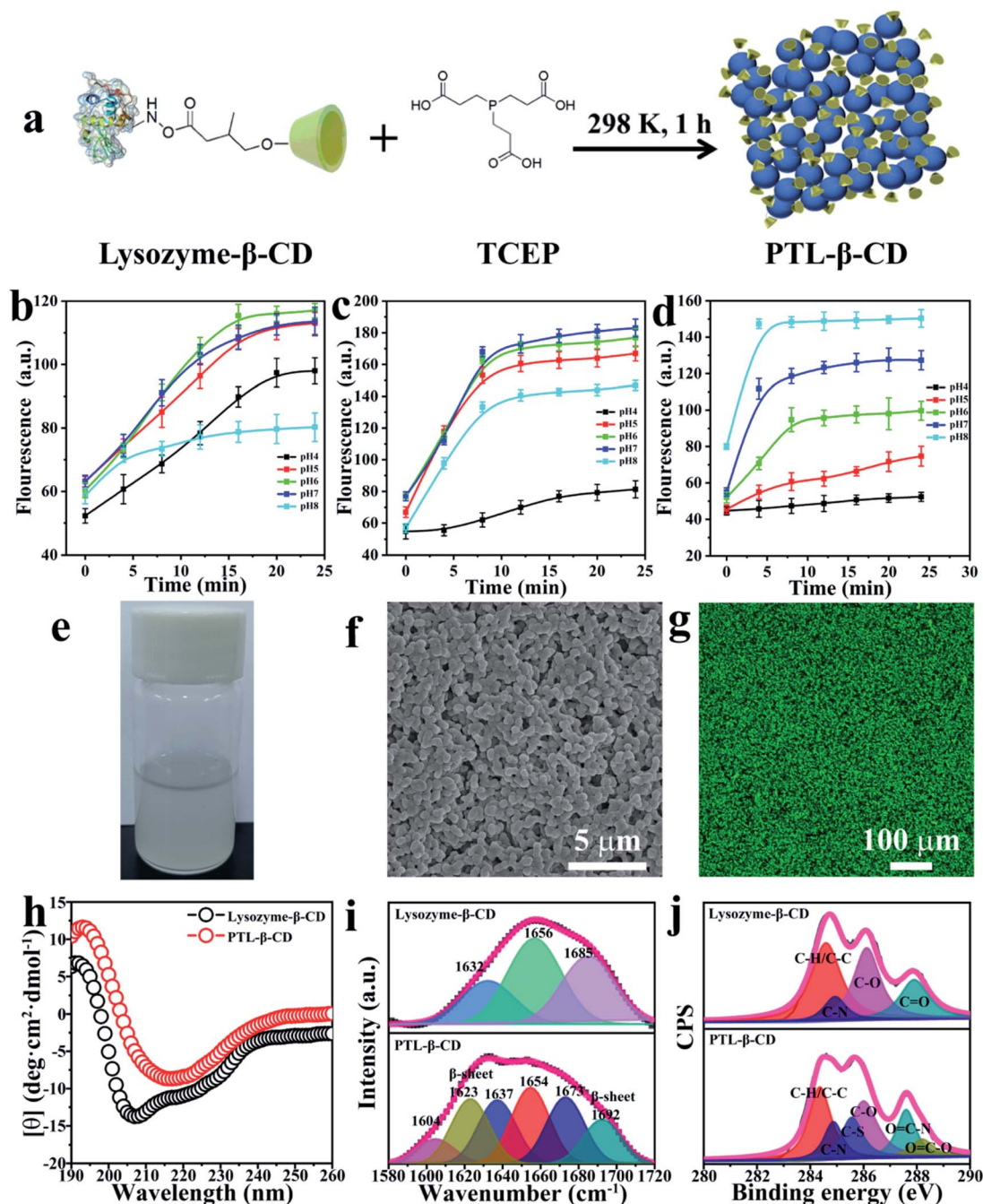


Fig. 2 Preparation and characterization of the PTL- β -CD aggregates. (a) Schematic preparation route of PTL- β -CD aggregates. The change of NPM (b), ANS (c), and ThT (d) fluorescence intensity of unfolded lysozyme- β -CD with time under different TCEP solution pH conditions. (e) Photograph of the obtained white solid PTL- β -CD aggregates. (f) SEM image of the PTL- β -CD aggregates. (g) Fluorescence microscopy image of the ThT stained PTL- β -CD aggregates. CD spectra (h) deconvolution of the FTIR amide I peak (i) and high-resolution C1s XPS spectra (j) of lysozyme- β -CD and PTL- β -CD. In cases of (e)–(j), lysozyme- β -CD (2 mg mL⁻¹) reacted with TCEP (50 mM, pH 7.0) for 2 hours.

NPM molecule could rapidly react with the free thiol to form a fluorescent derivative, which led to a fluorescence intensity enhancement at 380 nm.⁷⁹ The NPM fluorescence intensity of the mixed aqueous solution of lysozyme- β -CD and TCEP (pH 4.0, 5.0, 6.0, 7.0 or 8.0) rapidly increased and reached equilibrium within a few minutes (Fig. 2b), revealing that TCEP can break disulfide bonds in lysozyme- β -CD. The rupture of

disulfide bonds would further trigger unfolding of the lysozyme- β -CD conjugate, which was reflected by staining with the fluorescent dye 8-anilino-1-naphthalene-sulfonic acid (ANS).⁸⁰ ANS is a valuable probe for the detection of hydrophobic protein regions exposed upon unfolding; the corresponding fluorescence intensity at 475 nm of the mixture rapidly increased in approximately 20 min (Fig. 2c). This result implied a possible

conformational change during the breaking of the disulfide bonds in lysozyme- β -CD, which induced the exposure of the hydrophobic residue to enhance the fluorescence intensity resulting from ANS binding. Furthermore, the reaction process was monitored by thioflavin T (ThT) staining assay that has been widely utilized to recognize the β -sheet-rich structures of amyloid.⁸¹ As shown in Fig. 2d, the enhanced fluorescence intensity at 484 nm confirmed the formation of amyloid-like aggregates rich in β -sheet structures driven by hydrophobic forces during the phase transition process. Eventually, water-insoluble white PTL- β -CD aggregates mainly composed of nanoparticles and microparticles that could be stained by ThT were obtained in the bulk solution (Fig. 2e–g). Fig. 2h shows the far-CD spectra of lysozyme- β -CD and PTL- β -CD aggregates; the characteristic peaks of α -helix at 208 nm and 222 nm disappeared, and a typical single peak of β -sheet appeared at 216 nm in the latter spectrum, indicating the transformation of the secondary structure in lysozyme- β -CD and the formation of internal β -sheet stackings in PTL- β -CD aggregates, which was further supported by the FTIR results (Fig. 2i).

The specific surface area and surface chemical properties determine the adsorption performance of the adsorbents. Our previous work has reported that the TCEP solution pH significantly impacts the lysozyme phase transition process and finally the morphology of the phase-transited product.⁶³ Correspondingly, the effect of TCEP solution pH on the morphology and specific surface area of the PTL- β -CD aggregates was investigated. When the pH increased from 4.0 to 8.0, the morphologies of the PTL- β -CD aggregates changed obviously from plate to sphere with a distinguishable boundary between microparticles (Fig. S3†). The pore size distribution and specific surface area of the PTL- β -CD aggregates were evaluated through the Brunauer–Emmett–Teller (BET) method. The results suggested that the obtained aggregates mainly contained macropores inside (Fig. S4†), and their specific surface area increased first and then decreased. At pH 7.0, their specific surface area reached the maximum value of $8.4 \text{ m}^2 \text{ g}^{-1}$ (Fig. S5†). Because of the attenuation of electrostatic repulsion among the colloids, amyloid aggregation was enhanced by increasing the pH to approach the pI of the protein (about 10 for lysozyme- β -CD, Fig. S6†). The XPS test was employed to analyse the surface chemical state. Fig. S7† shows that the main elements on the surface of PTL- β -CD aggregates are C, O, N and S, and the deconvoluted C_{1s} spectra in Fig. 2j further indicate that there are various chemical groups including α -carbon (C–H/C–C), amine (C–N), hydroxyl (C–O), mercaptan (C–S), amide (O=C–N), and carboxyl (O=C–O) on the surface of PTL- β -CD aggregates. These exposed chemical groups possibly provide active sites for subsequent uranium ion adsorption.

2.3. Factors affecting uranium ion adsorption by the PTL- β -CD aggregates

The solution pH can change both the form of metal ions and the adsorbent surface charge distribution, which further influence the interaction between them. Therefore, the effect of aqueous solution pH on uranium ion adsorption by PTL- β -CD aggregates

was systematically studied. As can be seen in Fig. 3a, the adsorption capacity of the PTL- β -CD aggregates increased rapidly from pH 2.8 to pH 6.0 and then decreased with further increase in the solution pH; the maximum uptake of 9.03 mg g^{-1} was achieved at pH 6.0 after adsorption for 24 h. At the point of pH 8.0, which falls within the pH range of natural seawater, the PTL- β -CD aggregates have an adsorption capacity of 7.36 mg g^{-1} , suggesting the possibility of this adsorbent for uranium extraction from natural seawater. When the solution pH is lower than 6.0, the main forms of uranium ions are UO_2^{2+} , $\text{UO}_2(\text{OH})^+$, and $\text{UO}_2(\text{OH})_2$,^{57,58} and the PTL- β -CD surface is highly protonated and positively charged (Fig. S8†). The free UO_2^{2+} and $\text{UO}_2(\text{OH})^+$ have to compete with protons for binding sites; meanwhile, there is strong electrostatic repulsion between uranium ions and the PTL- β -CD surface; thus relatively poor adsorption was obtained at low solution pH. With the increase of pH to 6.0–7.0, the PTL- β -CD surface is progressively deprotonated, and the net charge is close to zero (Fig. S8†); the electrostatic repulsion effect decreased, and the main forms of uranium ions are $\text{UO}_2(\text{OH})^+$, $\text{UO}_2(\text{OH})_2$, and UO_2CO_3 ,^{57,58} the maximum adsorption capacity in this pH range is possibly attributed to electrostatic attraction and surface complexation between PTL- β -CD and uranium ions, which is in-depth analyzed in the following section involving the adsorption mechanism. As the pH increased continually, uranium ions form negatively charged complex anions, such as $\text{UO}_2(\text{CO}_3)_2^{2-}$, $\text{UO}_2(\text{OH})_3^-$ and $\text{UO}_2(\text{CO}_3)_3^{4-}$.^{57,58} The electrostatic repulsion between the negatively charged PTL- β -CD (Fig. S8†) and uranium ions lowered the adsorption capability.

The pH and concentration of TCEP solution, which determine the physical structure of the PTL- β -CD aggregates (Fig. S3–S5†), could influence their adsorption properties. Fig. 3b presents the adsorption capacity of the PTL- β -CD aggregates prepared under different TCEP solution pH conditions. It is clearly shown that the maximum adsorption capacity of 7.2 mg g^{-1} is obtained at pH 7.0 which is consistent with the BET result, in which the adsorbent has the maximum specific surface area at pH 7.0 (Fig. S5†). With increasing TCEP concentration from 10 mM to 100 mM, the adsorption capacity of PTL- β -CD aggregates increased rapidly and stabilized at approximately 50 mM (Fig. 3c). Therefore, in the subsequent experiments, the pH value and concentration of TCEP solution were set at 7.0 and 50 mM to prepare PTL- β -CD aggregates, respectively.

The adsorption time and initial uranium ion concentration are also essential for adsorption performance. As shown in Fig. 3d and S9,† the adsorption capacity increased rapidly at the beginning and then tended to stabilize gradually during the adsorption process; in addition, the higher the initial uranium ion concentration, the longer the time needed to reach equilibrium, and a larger adsorption capacity could be obtained. In particular, the adsorption capacity of the PTL- β -CD aggregates is 7 times higher than that of the PTL aggregates without grafting β -CD (Fig. S10†), which indicated that the excellent adsorption performance of the PTL- β -CD aggregates mainly resulted from β -CD. These results illustrated that the combination of β -CD and lysozyme amyloid-like aggregation is an

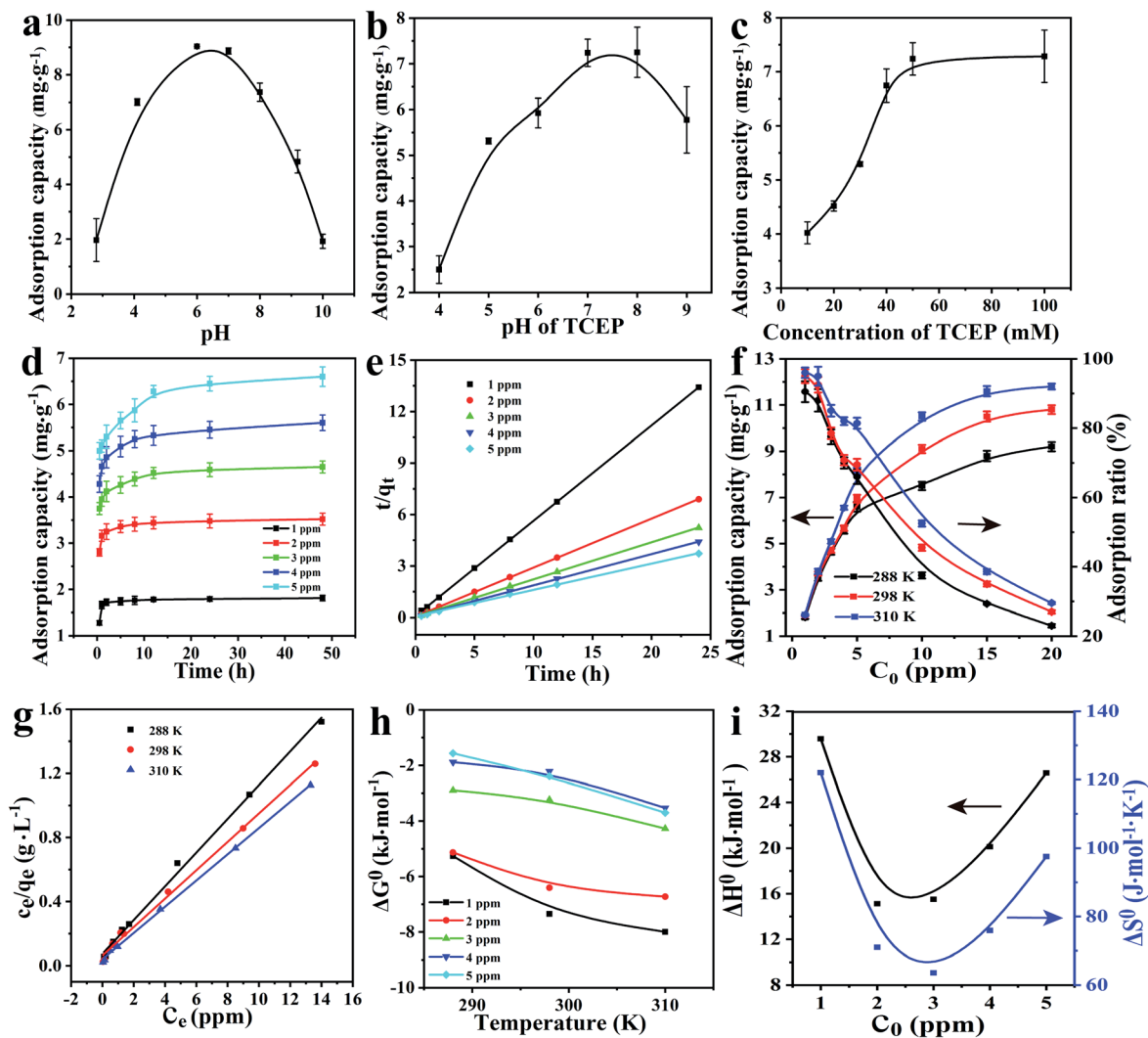


Fig. 3 (a) The uranium ion adsorption capacity of PTL- β -CD in the solutions with different pH. The uranium ion adsorption capacity of PTL- β -CD prepared under different TCEP solution pH conditions (b) and concentrations (c). (d) Time dependent adsorption capacity of PTL- β -CD at different initial uranium ion concentrations. (e) Pseudo-second-order kinetic fitting for the adsorption of uranium ions by PTL- β -CD. (f) The uranium adsorption ratio and corresponding adsorption capacity on PTL- β -CD as a function of the concentration of uranium ions at different temperatures. (g) Langmuir isotherm fitting for the adsorption of uranium ions onto PTL- β -CD. Thermodynamic parameters of uranium ion adsorption on PTL- β -CD, including the changes in Gibbs free energy (ΔG^0) (h), enthalpy (ΔH^0) (i) and entropy (ΔS^0) (i).

efficient strategy to develop an effective proteinaceous uranium ion adsorbent.

2.4. Kinetic and thermodynamic analyses of the adsorption

Adsorption kinetic experiments were carried out, and the data of uranium ion adsorption by PTL- β -CD aggregates at different times were fitted with pseudo-first order and pseudo-second order rate models to study the physicochemical process and the kinetic mechanism of adsorption (Fig. S11,[†] and 3e). The kinetic parameters are given in Table S1.[†] It is found that the correlation coefficient of pseudo-second-order kinetics (R_2^2) is higher than that of pseudo-first-order kinetics (R_1^2), indicating that chemical adsorption through complexation is the main mechanism of uranium ion adsorption by PTL- β -CD

aggregates, and the adsorption process is mainly controlled by the chemical reaction. The interaction between the adsorbate and adsorbent as well as the adsorption capacities of adsorbents can be reflected by adsorption isotherms. Here, with the change of temperature from 288 K to 310 K, the adsorption capacity of PTL- β -CD for uranium ions increased from 9.2 mg g⁻¹ to 11.8 mg g⁻¹. The equilibrium adsorption capacity of uranium ions is positively correlated with temperature (Fig. 3f), demonstrating that elevated temperature could enhance adsorption probably due to the increase in surface activity and kinetic energy of the solute. Furthermore, these adsorption data were fitted by the Langmuir and Freundlich isotherm models, respectively. It is found that compared to the Freundlich adsorption isotherm model, the Langmuir adsorption isotherm model is more suitable for describing the

adsorption process of uranium ions on the PTL- β -CD aggregates (Fig. 3g, S12, and Table S2[†]), revealing that this adsorption process is a homogeneous single layer adsorption process. Thermodynamic parameters such as Gibbs free energy change (ΔG^0), enthalpy change (ΔH^0) and entropy change (ΔS^0) provide valuable information with respect to the adsorption mechanism. The van't Hoff equation is used to calculate the free energy change ΔG^0 ($\Delta G^0 = -RT \ln K_C$, K_C is the distribution coefficient) reflecting the adsorption state of the adsorbate on the adsorbent surface and the spontaneity and feasibility of the adsorption process. As shown in Fig. 3h and Table S3,[†] at low uranium ion concentrations (e.g., 1–5 ppm), the ΔG^0 is negative at all tested temperatures (288 K, 298 K and 310 K), which indicated spontaneous adsorption on the PTL- β -CD aggregate surface. With an increase in the initial uranium ion concentration, more uranium ions were adsorbed on the PTL- β -CD aggregates, fewer adsorption sites were left and the ΔG^0 increased correspondingly. ΔH^0 and ΔS^0 were further derived from the intercept and slope of the plot of ΔG^0 versus T (Gibbs–Helmholtz equation, $\Delta G^0 = \Delta H^0 - T\Delta S^0$) (Fig. 3i and Table S3[†]). The positive ΔH^0 indicates that the adsorption is an endothermic process, and the increase in temperature is beneficial for the adsorption, which is consistent with the experimental results (Fig. 3f). The positive ΔS^0 shows that the adsorption of uranium ions on the adsorbent is a spontaneous adsorption process with high chemical affinity and also reflects the increase of randomness of the solid solution interface in the adsorption process. It is indicated that the adsorption of uranium ions on the adsorbent is entropically driven. During the adsorption process, uranium ions exchanged with water molecules on the aggregates' surface, and the entropy became positive as a result of the desorption of water molecules.

2.5. Selective adsorption of uranium ions by the PTL- β -CD aggregates

Practically, there are a large number of competing metal ions in natural seawater and wastewater interfering with the separation and recovery of uranium ions by adsorbents; many efforts have been made to improve the uranium ion adsorption selectivity.^{29–34} In order to evaluate the selectivity of the PTL- β -CD aggregates, a solution containing various metal ions (e.g., UO_2^{2+} , VO^{2+} , Cr^{3+} , Fe^{3+} , Mn^{2+} , Ni^{2+} , Pb^{2+} , Cd^{2+} , Co^{2+} , Mg^{2+} , As^{3+} , K^+ , Ca^{2+} , and Na^+) with a concentration of 1 ppm each was used. The adsorption ratio of uranium ions (95.05%) by the PTL- β -CD aggregates was significantly higher than that of other elements, especially the vanadium ion (1.18%) which is the main competitive metal ion of the uranium ion in natural seawater (Fig. 4a). The selective ratio of the PTL- β -CD aggregates for uranium ions to vanadium ions is 4–60 times higher than that of the other existing reported materials (such as nanofibers, DNA nano-pockets, polymeric peptides, and protein fibers).^{29–34} The main reason for the high selectivity towards uranium ions is that β -CD has a higher binding free energy for uranium ions ($-29.95 \text{ kcal mol}^{-1}$) compared to other metal ions (e.g., Li, $-14.45 \text{ kcal mol}^{-1}$; Na, $-15.51 \text{ kcal mol}^{-1}$; K, $-17.43 \text{ kcal mol}^{-1}$; Rb, $-19.01 \text{ kcal mol}^{-1}$; Mg,

$-26.99 \text{ kcal mol}^{-1}$; Ca, $-22.76 \text{ kcal mol}^{-1}$; Sr, $-23.61 \text{ kcal mol}^{-1}$; Ba, $-26.84 \text{ kcal mol}^{-1}$).^{46,47} In addition to metal cations, the effect of the most common concomitant anions including Cl^- , CO_3^{2-} , NO_3^- and SO_4^{2-} on uranium ion adsorption was also studied. As shown in Fig. 4b, these anions had a limited effect on uranium ion adsorption. Moreover, the adsorption capacity of PTL- β -CD aggregates in a solution with 3.3 ppb uranium ion concentration that mimics natural seawater was examined. It is calculated, according to the uranium ion concentration before and after adsorption, that the PTL- β -CD aggregates exhibit a high adsorption ratio of 87% in the ultralow uranium ion concentration solution (Fig. 4c). The above results suggested that the PTL- β -CD aggregates have potential applications in uranium extraction from seawater or nuclear industrial wastewater.

2.6. Mechanism of uranium ion adsorption by the PTL- β -CD aggregates

The elements on the surface of the PTL- β -CD aggregates before and after adsorption were characterized by XPS. Compared to the native PTL- β -CD aggregates (Fig. S7[†]), an obvious characteristic peak at 390.0 eV belonging to uranium was observed in the XPS spectrum of the PTL- β -CD aggregates after adsorption (Fig. S13[†]), which indicated the successful uptake of uranium ions on PTL- β -CD aggregates' surface. The small shoulder peaks at 390.9 eV and 379.6 eV in the high-resolution XPS spectra of U_{4f} (Fig. 4d) reflected that some of U(vi) adsorbed on PTL- β -CD aggregates was reduced to U(IV).¹⁵ The possible mechanisms for the reduction of uranium ions include the following two aspects^{82–84} (1) dehydrogenation of aliphatic hydrocarbon moieties ($\text{RH}_2 + \text{UO}_2^{2+} = \text{R} + \text{UO}_2 + 2\text{H}^+$) and (2) oxidation of hydroxyl groups on the PTL- β -CD aggregates' surface (e.g., phenolic hydroxyl of tyrosine: $-\text{CH}-\text{OH} + \text{UO}_2^{2+} = -\text{C}=\text{O} + \text{UO}_2 + 2\text{H}^+$). The mechanism of uranium ion adsorption by PTL- β -CD was thoroughly analyzed from the FTIR and XPS spectra of high-resolution C_{1s} , N_{1s} , and O_{1s} , respectively. After PTL- β -CD adsorbed uranium ions, the C–O and N–C=O peaks appeared at the lower binding energy, indicating that a variety of oxygen functional groups may participate in the electrostatic attraction with uranium ions during the adsorption process (Fig. 4e). The spectral area of the protonated N_{1s} was significantly reduced after the adsorption of uranium ions by PTL- β -CD (Fig. 4f), implying electrostatic interaction between protonated amino groups (such as arginine residues) and uranium ions. The presence of a new peak at 531.35 eV owing to the O=U=O group on the O_{1s} spectrum of the PTL- β -CD surface after adsorption (Fig. 4g) further indicated that the uranyl was mainly complexed with the hydroxyl groups on β -CD.^{6,15} In the FTIR spectra, a new peak corresponding to the antisymmetric stretching vibration mode of O=U=O which appeared at 905 cm^{-1} after the adsorption of uranium ions on PTL- β -CD also suggested the complexation between uranium ions and the adsorbent (Fig. S14[†]). Additionally, it could be noticed in the FTIR spectra that the band of the valence vibration of –OH in PTL- β -CD was shifted from 3360 cm^{-1} to 3450 cm^{-1} after adsorbing uranium ions (Fig. S14[†]), which was ascribed to the

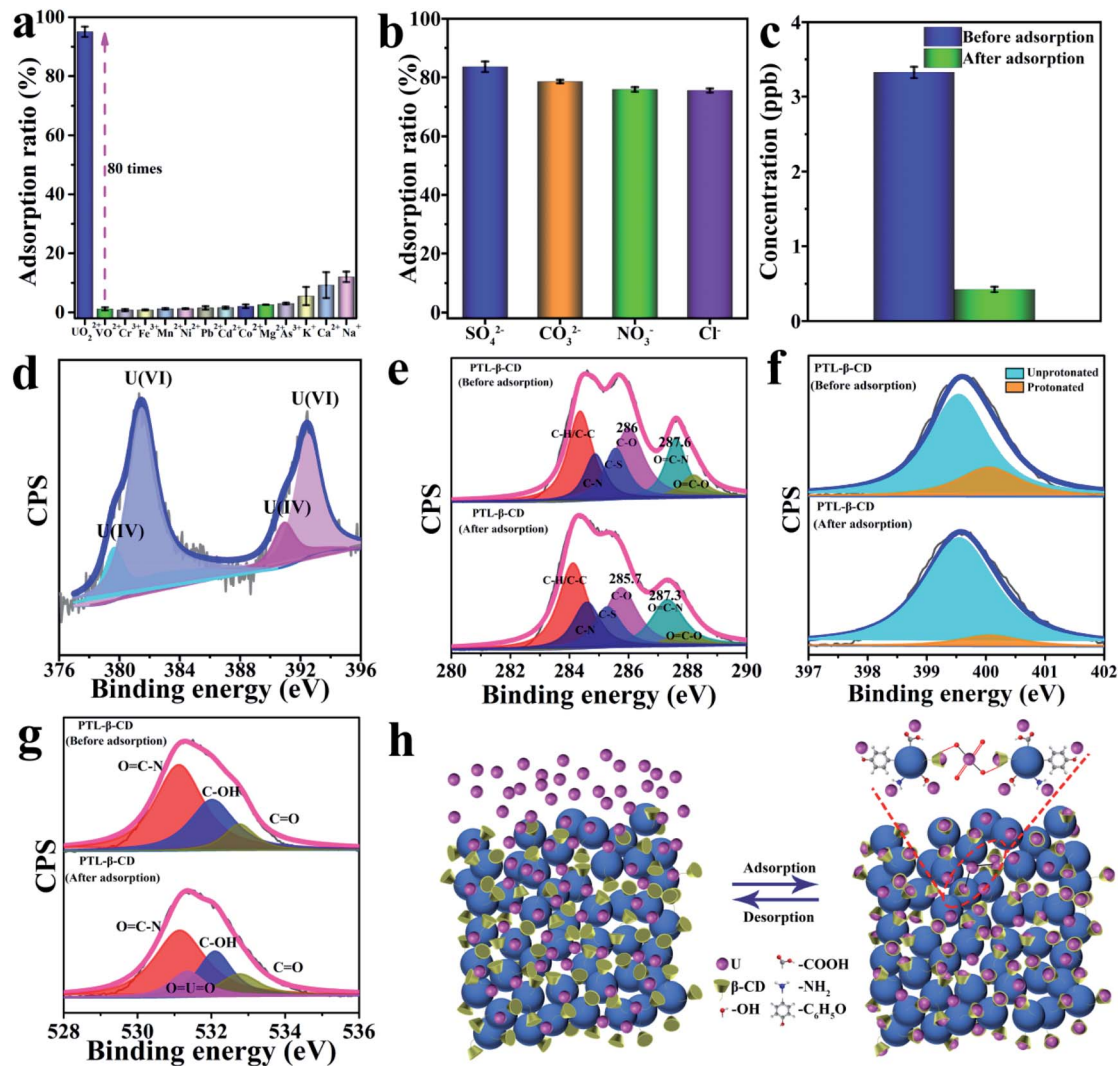


Fig. 4 (a) The effect of competing metal ions (1 ppm each) on uranium ion adsorption. (b) The effect of Cl^- , CO_3^{2-} , SO_4^{2-} and NO_3^- (0.01 M) on uranium ion adsorption. (c) The adsorption capacity of PTL- β -CD in a solution with 3.3 ppb uranium ion concentration that mimics natural seawater. High-resolution XPS spectra of U_{4f} (d), C_{1s} (e), N_{1s} (f), and O_{1s} (g) on the PTL- β -CD surface before and after adsorption of uranium ions. (h) Schematic illustration of the uranium ion adsorption–desorption process by PTL- β -CD.

host–guest interaction between the hydrophobic cavity of β -CD and uranium ions resulting in a complete water release from the cavity.^{39–42} Compared with white PTL- β -CD aggregates, the color of PTL- β -CD aggregates that adsorbed uranium ions is faint yellow, and the color change has no influence on the structural intactness of the material (Fig. S15a and S16†). The existence of functional groups facilitated the gradually pronounced distribution of uranium on the PTL- β -CD aggregates, as reflected by SEM and corresponding energy dispersive spectroscopy (EDS) mapping of C, N, O, S and U on the PTL- β -CD aggregates (Fig. S15, S17 and Table S4†). Taken together, the above collected evidence then supported that the PTL- β -CD aggregates adsorb uranium ions mainly through electrostatic interaction, surface complexation (*e.g.*, defined host–guest interaction and metal chelation) and *in situ* reduction (Fig. 4h).

2.7. Commercialization prospects of the PTL- β -CD aggregates

The structural stability of materials plays an important role in their practical applications; thus we tested the structural intactness of PTL- β -CD under treatment with ultrasound, organic solvents, and extreme pH solutions. No obvious structural destruction can be observed in the SEM images of PTL- β -CD after treatment under these various conditions (Fig. S18†). In order to recover uranium ions from the adsorbent and enhance its durability for reducing the cost, cyclic adsorption–desorption experiments of the PTL- β -CD aggregates were performed. The uranium ion loaded PTL- β -CD aggregates were treated with the eluent solution of 1 M HNO_3 to desorb the uranium ions. As shown in Fig. 5a, after ten adsorption–desorption cycles, the adsorption ratio of the regenerated PTL- β -CD towards uranium ions was still higher than 90%, and the

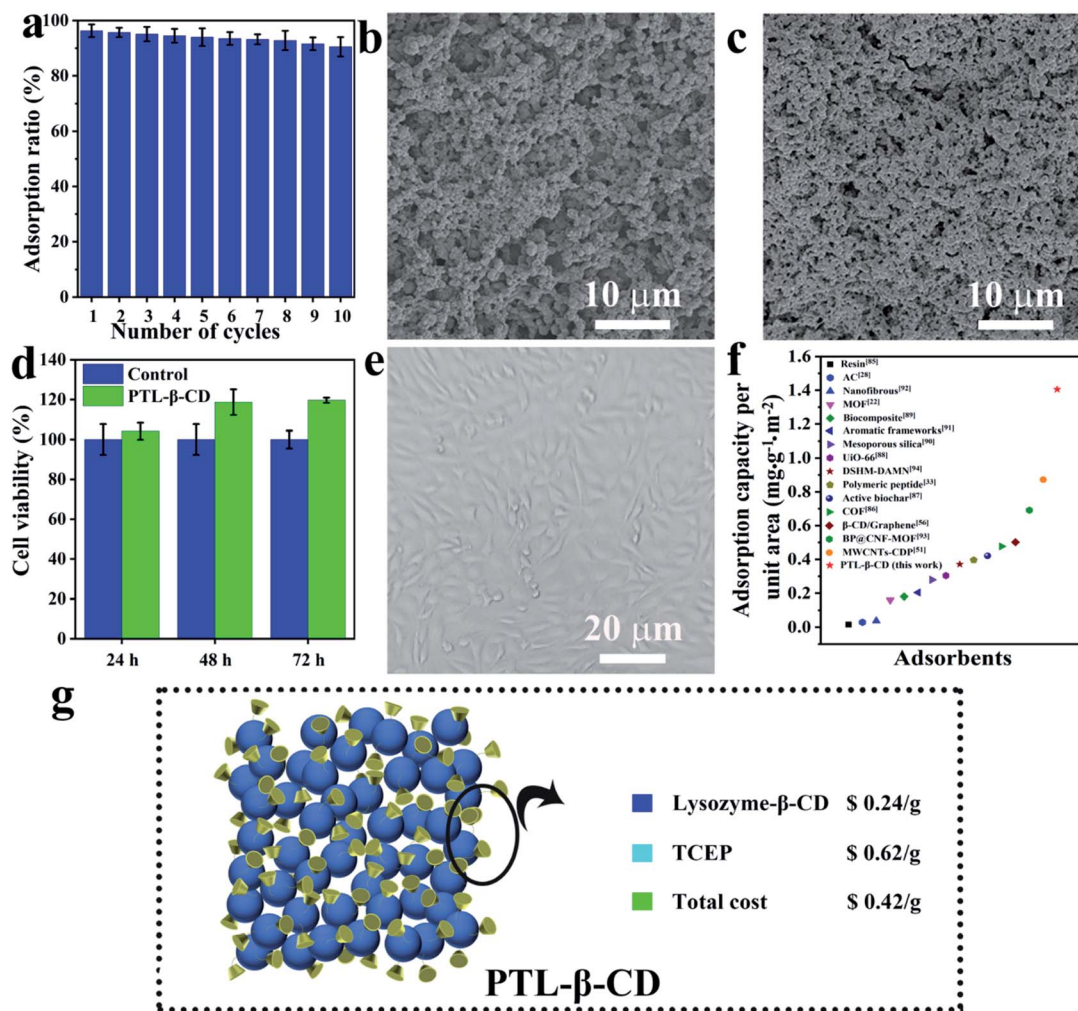


Fig. 5 (a) Cycles of uranium ion adsorption by the PTL-β-CD aggregates. SEM images of PTL-β-CD before uranium ion adsorption (b) and after uranium ion desorption (c). (d) The cell viability after co-culturing with PTL-β-CD for 24, 48 and 72 hours. (e) Microphotograph of the cell morphology after co-culturing with PTL-β-CD for 72 hours. (f) Comparison of the uranium ion adsorption capacity per unit area of different adsorbents (such as resins, AC, metal organic frameworks (MOFs), covalent organic frameworks (COFs), PTL-β-CD, etc.). (g) Scheme and material cost analysis of the PTL-β-CD system for uranium ion adsorption.

morphology and molecular weight of PTL-β-CD exhibited no obvious change (Fig. 5b, c and S19, S20†). In the more complex simulated seawater situation, PTL-β-CD could still maintain its morphology and structural stability after immersion for 30 days (Fig. S21†). The strong structural stability of the PTL-β-CD aggregates is largely attributed to the internal amyloid-like structure with enriched β-sheet stackings.^{69,70} The most currently developed uranium ion adsorbents such as inorganic materials, organic polymers, carbon family materials and porous framework materials are generally nondegradable and cause secondary environmental pollution. Because lysozyme and β-CD are widely used biomacromolecules, it is presumed that the developed proteinaceous adsorbent PTL-β-CD is friendly toward the environment and ecosystem. First, the MTT cell viability test of 3T3 cells was used to study the *in vitro* cytotoxicity of PTL-β-CD. After being co-cultured with the PTL-β-CD aggregates for 24, 48, and 72 hours, the 3T3 cells maintained good activity (Fig. 5d and S22†) and morphology (Fig. 5e),

indicating that PTL-β-CD has excellent biocompatibility and is expected to be harmless to the ecosystem. Moreover, it should be noted that even though the PTL-β-CD aggregates maintained structural integrity during the process of reuse, they could be ultimately degraded by protease. As shown in Fig. S23–S25,† all the native PTL-β-CD, uranium ion adsorbed PTL-β-CD and uranium ion desorbed PTL-β-CD could be completely degraded after incubation with trypsin for 2 h at 37 °C, providing a green method to treat this adsorbent at the end of its service life without producing secondary pollution that is always caused by landfilling or burning. Compared with the reported alternatives,^{85–94} the adsorbent PTL-β-CD possesses better performance in terms of adsorption capacity per unit area ($1.405 \text{ mg g}^{-1} \text{ m}^{-2}$) (Fig. 5f and Table S5†); this value is 3–90 times greater than those of ion exchange resins,⁸⁵ AC,²⁸ metal organic frameworks (MOFs)²² and covalent organic frameworks (COFs).⁸⁶ Except for the high adsorption, the cost of PTL-β-CD is also relatively low and is calculated to be only \$0.42 per g (Fig. 5g) which can fully

meet large-scale applications. In addition to the advantageous adsorption capacity and price, the fast kinetics, high selectivity and mild preparation/regeneration conditions, as well as environmental friendliness make this developed proteinaceous adsorbent have promising application in the field of metal ion extraction.

3. Conclusions

In summary, β -CD molecules were grafted onto lysozyme through the reaction of an amine with an *N*-succinimidyl activated ester, and the obtained lysozyme- β -CD conjugates could undergo an amyloid-like aggregation process to form solid PTL- β -CD aggregates in an all-aqueous environment without using toxic additives. These aggregates composed of micro-particles could be used to recover the uranium ions with high efficiency and selectivity. The adsorption mechanism is generally regarded to comprise physicochemical interactions between uranium ions and the functional groups present on the surface of the PTL- β -CD aggregates, typically including electrostatic interactions, metal ion chelation or complexation (between β -CD and uranium ions) and *in situ* reduction. The proteinaceous adsorbent showed a high adsorption ratio of 95.05% in the presence of various competing metal ions and anions indicating outstanding uranium ion selectivity and can be used for multiple cycles of adsorption-desorption. The adsorption capacity per unit area reached up to $1.405 \text{ mg g}^{-1} \text{ m}^{-2}$, which is 3–90 times higher than those of ion exchange resins, active carbon, organic frameworks and metal organic frameworks. Moreover, the PTL- β -CD aggregates have good biocompatibility and enzymatic degradability. This research highlights the potential application of a green technology for the economic extraction of uranium ions from aqueous medium using an adsorbent prepared from widely used biomolecules, which can efficiently reduce secondary pollution and realize the recycling economy and the reuse of biological resources.

Conflicts of interest

There are no conflicts to declare.

Acknowledgements

P. Y. is grateful for funding from the National Key R&D Program of China (No. 2020YFA0710400 and 2020YFA0710402), the National Natural Science Foundation of China (No. 21875132, 51903147), the 111 Project (No. B14041), the Fundamental Research Funds for the Central Universities (No. GK201801003), the Innovation Capability Support Program of Shaanxi (No. 2020TD-024), and the Science and Technology Innovation Team of Shaanxi Province (No. 2022TD-35). J. Z. appreciates funding from the National Natural Science Foundation of China (No. 51903146), the Natural Science Foundation of Shaanxi Province (No. 2020JQ-420), and the National Key R&D Program of China (No. 2020YFA0710400 and 2020YFA0710403).

References

- 1 M. L. Feng, D. Sarma, X. H. Qi, *et al.*, *J. Am. Chem. Soc.*, 2016, **138**, 12578–12585.
- 2 L. He, S. Liu, L. Chen, *et al.*, *Chem. Sci.*, 2019, **10**, 4293–4305.
- 3 Y. Yuan, B. Niu, Q. Yu, *et al.*, *Angew. Chem., Int. Ed.*, 2020, **59**, 1220–1227.
- 4 W. R. Cui, F. F. Li, R. H. Xu, *et al.*, *Angew. Chem., Int. Ed.*, 2020, **132**, 17837–17843.
- 5 L. Zhou, M. Bosscher, C. Zhang, *et al.*, *Nat. Chem.*, 2014, **6**, 236–241.
- 6 Q. Sun, B. Aguila, J. Perman, *et al.*, *Nat. Commun.*, 2018, **9**, 1–9.
- 7 M. J. Manos and M. G. Kanatzidis, *J. Am. Chem. Soc.*, 2012, **134**, 16441–16446.
- 8 S. O. Odoh, G. D. Bondarevsky, J. Karpus, *et al.*, *J. Am. Chem. Soc.*, 2014, **136**, 17484–17494.
- 9 R. V. Davies, J. Kennedy, R. W. McIlroy, *et al.*, *Nature*, 1964, **203**, 1110–1115.
- 10 Y. Suzuki, S. D. Kelly, K. M. Kemner, *et al.*, *Nature*, 2002, **419**, 134.
- 11 C. Liu, P. C. Hsu, J. Xie, *et al.*, *Nat. Energy*, 2017, **2**, 1–8.
- 12 B. Yan, C. Ma, J. Gao, *et al.*, *Adv. Mater.*, 2020, **32**, 1906615.
- 13 A. S. Ivanov, B. F. Parker, Z. Zhang, *et al.*, *Nat. Commun.*, 2019, **10**, 1–7.
- 14 X. Xu, H. Zhang, J. Ao, *et al.*, *Energy Environ. Sci.*, 2019, **12**, 1979–1988.
- 15 W. Luo, G. Xiao, F. Tian, *et al.*, *Energy Environ. Sci.*, 2019, **12**, 607–614.
- 16 C. W. Abney, R. T. Mayes, T. Saito, *et al.*, *Chem. Rev.*, 2017, **117**, 13935–14013.
- 17 S. E. Bone, J. J. Dynes, J. Cliff, *et al.*, *Proc. Natl. Acad. Sci. U. S. A.*, 2017, **114**, 711–716.
- 18 Y. Xie, C. Chen, X. Ren, *et al.*, *Prog. Mater. Sci.*, 2019, **103**, 180–234.
- 19 G. Zhu, *Chem*, 2021, **7**, 277–278.
- 20 Z. Li, F. Chen, L. Yuan, *et al.*, *Chem.–Eur. J.*, 2012, **210**, 539–546.
- 21 A. M. Starvin and T. P. Rao, *Talanta*, 2004, **63**, 225–232.
- 22 M. Carboni, C. W. Abney, S. Liu, *et al.*, *Chem. Sci.*, 2013, **4**, 2396–2402.
- 23 Y. Yue, R. T. Mayes, J. Kim, *et al.*, *Angew. Chem., Int. Ed.*, 2013, **125**, 13700–13704.
- 24 Z. Q. Bai, L. Y. Yuan, L. Zhu, *et al.*, *J. Mater. Chem. A*, 2015, **3**, 525–534.
- 25 C. Bai, J. Li, S. Liu, *et al.*, *Microporous Mesoporous Mater.*, 2014, **197**, 148–155.
- 26 B. Li, Q. Sun, Y. Zhang, *et al.*, *ACS Appl. Mater. Interfaces*, 2017, **9**, 12511–12517.
- 27 G. E. Fryxell, Y. Lin, S. Fiskum, *et al.*, *Environ. Sci. Technol.*, 2005, **39**, 1324–1331.
- 28 A. Mellah, S. Chegrouche and M. Barkat, *J. Colloid Interface Sci.*, 2006, **296**, 434–441.
- 29 D. Wang, J. Song, J. Wen, *et al.*, *Adv. Energy Mater.*, 2018, **8**, 1802607.

- 30 L. Feng, H. Wang, T. Feng, *et al.*, *Angew. Chem., Int. Ed.*, 2022, **61**, 82–86.
- 31 Y. Yuan, S. Feng, L. Feng, *et al.*, *Angew. Chem., Int. Ed.*, 2020, **132**, 4292–4298.
- 32 Y. Yuan, T. Liu, J. Xiao, *et al.*, *Nat. Commun.*, 2020, **11**, 1–8.
- 33 Y. Yuan, Q. Yu, M. Cao, *et al.*, *Nat. Sustain.*, 2021, **4**, 708–714.
- 34 Y. Yuan, Q. Yu, J. Wen, *et al.*, *Angew. Chem., Int. Ed.*, 2019, **131**, 11911–11916.
- 35 Q. Yu, Y. Yuan, L. Feng, *et al.*, *Angew. Chem., Int. Ed.*, 2020, **132**, 16131–16135.
- 36 S. V. Wegner, H. Boyaci, H. Chen, *et al.*, *Angew. Chem., Int. Ed.*, 2009, **48**, 2339–2341.
- 37 S. Kou, Z. Yang and F. Sun, *ACS Appl. Mater. Interfaces*, 2017, **9**, 2035–2039.
- 38 L. Zhou, M. Bosscher, C. Zhang, *et al.*, *Nat. Chem.*, 2014, **6**, 236–241.
- 39 G. Crini, *Chem. Rev.*, 2014, **114**, 10940–10975.
- 40 Y. Chen and Y. Liu, *Chem. Soc. Rev.*, 2010, **39**, 495–505.
- 41 V. J. Stella and Q. He, *Toxicol. Pathol.*, 2008, **36**, 30–42.
- 42 J. Zhang and P. X. Ma, *Adv. Drug Delivery Rev.*, 2013, **65**, 1215–1233.
- 43 B. Tian, S. Hua, Y. Tian, *et al.*, *Environ. Sci. Pollut. Res.*, 2021, **28**, 1317–1340.
- 44 N. Tarannum and D. Kumar, *J. Polym. Res.*, 2020, **27**, 1–30.
- 45 N. Morin-Crini and G. Crini, *Prog. Polym. Sci.*, 2013, **38**, 344–368.
- 46 N. Li, L. Yang, X. Ji, *et al.*, *Environ. Sci.*, 2020, **7**, 3124–3135.
- 47 N. Li, L. Yang, D. Wang, *et al.*, *Environ. Sci. Technol.*, 2021, **55**, 9181–9188.
- 48 A. Alsbaiee, B. J. Smith, L. Xiao, *et al.*, *Nature*, 2016, **529**, 190–194.
- 49 M. J. Klemes, Y. Ling, C. Ching, *et al.*, *Angew. Chem., Int. Ed.*, 2019, **131**, 12177–12181.
- 50 M. J. Klemes, L. P. Skala, M. Ateia, *et al.*, *Acc. Chem. Res.*, 2020, **53**, 2314–2324.
- 51 J. H. Xue, H. Zhang, D. X. Ding, *et al.*, *Ind. Eng. Chem. Res.*, 2019, **58**, 4074–4083.
- 52 W. C. Song, D. D. Shao, S. S. Lu, *et al.*, *Sci. China: Chem.*, 2014, **57**, 1291–1299.
- 53 W. Li, H. Liu, L. Li, *et al.*, *J. Radioanal. Nucl. Chem.*, 2019, **322**, 2033–2042.
- 54 S. Yang, P. Zong, J. Hu, *et al.*, *Chem. Eng. J.*, 2013, **214**, 376–385.
- 55 X. Hao, R. Chen, Q. Liu, *et al.*, *Inorg. Chem. Front.*, 2018, **5**, 2218–2226.
- 56 A. S. Helal, E. Mazario, A. Mayoral, *et al.*, *Environ. Sci.*, 2018, **5**, 158–168.
- 57 P. Zong, X. Xu, M. Shao, *et al.*, *Int. J. Hydrogen Energy*, 2021, **46**, 1370–1384.
- 58 J. Wang, R. Zhang, Z. Lu, *et al.*, *Ecol. Eng.*, 2020, **149**, 105835.
- 59 C. Ding, W. Cheng, Z. Jin, *et al.*, *J. Mol. Liq.*, 2015, **207**, 224–230.
- 60 J. Xiao, Y. Chen and J. Xu, *J. Ind. Eng. Chem.*, 2014, **20**, 2830–2839.
- 61 A. Shahmohammadi, *Eur. Food Res. Technol.*, 2018, **244**, 577–593.
- 62 T. Wu, Q. Jiang, D. Wu, *et al.*, *Food Chem.*, 2019, **274**, 698–709.
- 63 Z. Wei, S. Wu, J. Xia, *et al.*, *Biomacromolecules*, 2021, **22**, 890–897.
- 64 P. Yang, *Macromol. Biosci.*, 2012, **12**, 1053–1059.
- 65 Z. Wu and P. Yang, *Adv. Mater. Interfaces*, 2015, **2**, 1400401.
- 66 C. Li, L. Xu, Y. Y. Zuo, *et al.*, *Biomater. Sci.*, 2018, **6**, 836–841.
- 67 F. Yang, Z. Yan, J. Zhao, *et al.*, *J. Mater. Chem. A*, 2020, **8**, 3438–3449.
- 68 Q. Yang, J. Cao, F. Yang, *et al.*, *Chem.–Eur. J.*, 2021, **416**, 129066.
- 69 R. Liu, J. Zhao, Q. Han, *et al.*, *Adv. Mater.*, 2018, **30**, 1802851.
- 70 D. Wang, Y. Ha, J. Gu, *et al.*, *Adv. Mater.*, 2016, **28**, 7414–7423.
- 71 C. Li, R. Qin, R. Liu, *et al.*, *Biomater. Sci.*, 2018, **6**, 462–472.
- 72 J. Gu, S. Miao, Z. Yan, *et al.*, *Colloid Interface Sci. Commun.*, 2018, **22**, 42–48.
- 73 F. Yang, F. Tao, C. Li, *et al.*, *Nat. Commun.*, 2018, **9**, 1–11.
- 74 Y. Xu, Y. Liu, X. Hu, *et al.*, *Angew. Chem., Int. Ed.*, 2020, **59**, 2850–2859.
- 75 M. Chen, F. Yang, X. Chen, *et al.*, *Adv. Mater.*, 2021, **33**, 2104187.
- 76 Y. Liu, F. Tao, S. Miao, *et al.*, *Acc. Chem. Res.*, 2021, **54**, 3016–3027.
- 77 J. Gu, Y. Su, P. Liu, *et al.*, *ACS Appl. Mater. Interfaces*, 2017, **9**, 198–210.
- 78 K. Hussain, I. Ali, S. Ullah, *et al.*, *J. Cluster Sci.*, 2022, **33**, 339–348.
- 79 R. A. Winters, J. Zukowski, N. Ercal, *et al.*, *Anal. Biochem.*, 1995, **227**, 14–21.
- 80 E. Schönbrunn, S. Eschenburg and K. Luger, *Proc. Natl. Acad. Sci. U. S. A.*, 2000, **97**, 6345–6349.
- 81 S. S. S. Wang, K. N. Liu and B. W. Wang, *Eur. Biophys. J.*, 2010, **39**, 1229–1242.
- 82 F. Yang, Q. Yang, M. Chen, *et al.*, *Cell Rep. Phys. Sci.*, 2021, **2**, 100379.
- 83 H. Zhang, W. Liu, A. Li, *et al.*, *Angew. Chem., Int. Ed.*, 2019, **58**, 16110–16114.
- 84 S. Kushwaha, B. Sreedhar and P. Padmaja, *Langmuir*, 2012, **28**, 16038–16048.
- 85 J. Bai, X. Ma, C. Gong, *et al.*, *J. Mol. Liq.*, 2020, **320**, 114443.
- 86 Q. Sun, B. Aguila, L. D. Earl, *et al.*, *Adv. Mater.*, 2018, **30**, 1705479.
- 87 Q. Zhang, Y. Wang, Z. Wang, *et al.*, *J. Alloys Compd.*, 2021, **852**, 156993.
- 88 Q. Yu, Y. Yuan, J. Wen, *et al.*, *Adv. Sci.*, 2019, **6**, 1900002.
- 89 S. Aytas, D. A. Turkozu and C. Gok, *Desalination*, 2011, **280**, 354–362.
- 90 S. Yang, J. Qian, L. Kuang, *et al.*, *ACS Appl. Mater. Interfaces*, 2017, **9**, 29337–29344.
- 91 Y. Yuan, Y. Yang, X. Ma, *et al.*, *Adv. Mater.*, 2018, **30**, 1706507.
- 92 S. Xie, X. Liu, B. Zhang, *et al.*, *J. Mater. Chem. A*, 2015, **3**, 2552–2558.
- 93 M. Chen, T. Liu, X. Zhang, *et al.*, *Adv. Funct. Mater.*, 2021, **31**, 2100106.
- 94 J. Zhang, H. Zhang, Q. Liu, *et al.*, *Chem.–Eur. J.*, 2019, **368**, 951–958.